Supporting Information for

Optimization of passive acoustic bedload monitoring in rivers by signal inversion

Mohamad Nasr[1], Adele Johannot[1], Thomas Geay[2,3], Sebastien Zanker[4], Jules Le Guern[3], Alain Recking[1]

[1]University Grenoble Alpes, INRAE, ETNA, Grenoble, France.

[2] Office National des Forêts, service Restauration Terrain Montagne 38000 Grenoble, France.

[3] GINGER BURGEAP, R&D, 38000 Grenoble, France.

[4]EDF Hydro, DTG, 38950 Saint-Martin-le-Vinoux, France.

Additional Supporting Information (Files uploaded separately)

Recording samples and bedload flux data are presented in (Nasr, Mohamad; Johannot, Adele ; Geay, Thomas ; Zanker, Sebastien ; Recking, Alain; Le Guern, Jules (2022), "Optimization of passive acoustic bedload monitoring in rivers by signal inversion ", Mendeley Data, V1, doi: 10.17632/vygy6tsy5n.1)

Description

This supporting document provides the measured and inversed profiles (Figure S1-S24) for the data set from Geay et al. (2020) and which is used in section 4.2 of the manuscript. Figure S25 presentes a river slope-based empirical equation to predict the attenuation coefficient of rives.

S1. Measured and inversed acoustic profiles

This section presents the dataset for the global calibration curves (Geay et al., 2020), and inversed global calibration curve presented section 6.2 in the manuscript. Table S1 summarizes each river's characteristics and measured values of bedload flux and acoustic power. Figures S1-S24 present the measured and inversed acoustic power profiles for each river

Table S1. A summary of the measured sites of (Geay et al., 2020) and their corresponding characteristics. Where S is the local slope of the river, W is the width of the river section, $\alpha_{\lambda c}$ is the attenuation coefficient for the spherical model, H is the average water level, V is the average flow velocity, $\overline{q_s}$ and $\overline{P}$ are the cross-sectional average specific bedload flux and acoustic power respectively.

River	Location	S (m/m)	W (m)	$\alpha_{\lambda,s}$	Symbol	H (m)	V (m/s)	Bedload GSD		$\overline{q_s}$ (g/s/m)	$\overline{P}$ (10^{12} μPa^2)	$\overline{P}$ inversed (10^{12} μPa^2/
								D50	D84			
Arve	Bossons	0.0075	14	0.096	AR1	1.35	2.01	1.4	6.4	157.7	14.06	4.54
					AR2	1.2	1.73	1.4	4.6	60.1	3.30	1.05
Giffre	Samoëns	0.003	31	0.0074	GI	0.9	1.83	6.8	58.8	328.2	550.52	37.31
GrandBuech	La Faurie	0.007	13.5	0.04	GB1	0.65	1.65	40.8	69.8	30.8	6.76	0.36
					GB2	0.69	1.75	19.3	63.5	16.9	9.70	0.74
Isère	Campus	0.0005	60	~0	IC	2.8	1.41	2.0	14.4	32.7	11.90	0.58
Moselle	Bainville-aux-Miroirs	0.0011	16	0.006	MO	2.8	1.94	19.6	46.6	379.3	141.68	12.03
Romanche	Le Bourg d Oisans/Centre	0.0013	33	0.005	RO	1.2	1.39	0.9	2.9	53.9	33.38	1.54
Sarenne		0.0013	8	0.005	SA1	0.44	1.05	3.3	11.4	31.6	3.41	0.10

River	Location	S (m/m)	W (m)	$\alpha_{\lambda,s}$	Symbol	H (m)	V (m/s)	Bedload GSD		$\overline{q_s}$ (g/s/m)	$\overline{P}$ (10^{12} μPa^2)	$\overline{P}$ inversed (10^{12} $\mu Pa^2/$
								D50	D84			
	Le Bourg-d Oisans/ Pont de Bassey				SA2	0.49	0.97	5.8	15.2	32.4	5.22	0.17
					SA3	0.46	0.92	-	-	2.3	1.36	0.06
Selves	Le Puech	0.025	10	0.14	Sel	0.98	1.61	2.9	7.1	14.3	0.28	0.09
Séveraisse	Villar Loubiére	0.011	12.5	0.055	SVL1	0.7	1.65	5.1	48.5	75.4	26.77	2.76
					SVL2	0.75	1.53	11.3	52.8	41.1	11.88	1.55
					SVL3	0.76	1.63	38.8	75.1	48.2	33.19	4.71
					SVL4}	0.88	1.57	54.3	77.4	111.3	50.90	6.70
					SVL5	0.82	1.48	62.1	87.2	63.7	5.79	0.51
					SVL6	0.73	1.79	0.0	0.0	11.9	0.96	0.17
	La Chapelle	0.0145	14	0.02	SLC1	0.46	2.06	0.0	0.0	44.9	3.76	0.17
					SLC2	0.36	2.03	23.4	75.1	74.9	16.60	0.46
					SLC3	0.37	1.56	0.0	0.0	8.7	1.62	0.06
Garonne	Pont Du Roy	0.003	22	0.003	GPR	1.63	1.88	3.5	15.1	58.9	5.26	0.19
	Saint-Béat	0.0041	32	0.006	GSB	1.25	2.31	3.5	12.5	80.1	45.79	3.60
Gave de Gavarnie	Villelongue	0.003	27	0.003	GG	0.7	1.70	1.9	6.1	1.2	1.97	0.10

River	Location	S (m/m)	W (m)	$\alpha_{\lambda,s}$	Symbol	H (m)	V (m/s)	Bedload GSD		$\overline{q_s}$ (g/s/m)	$\overline{P}$ (10^{12} μPa^2)	$\overline{P}$ inversed (10^{12} μPa^2/
								D50	D84			
Gave de Pau	Ayzac-Ost	0.003	35.3	0.003	GP	1.53	2.50	3.9	35.8	41.0	23.30	1.02

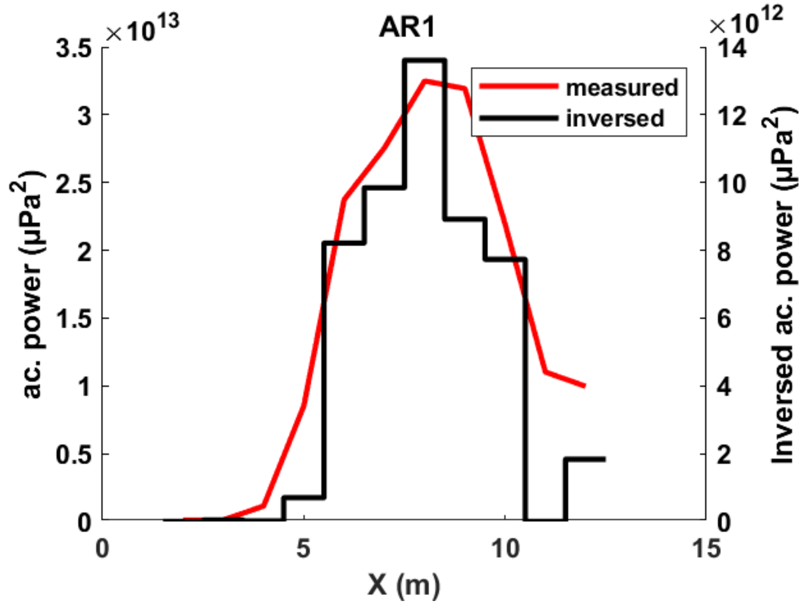

Figure S1

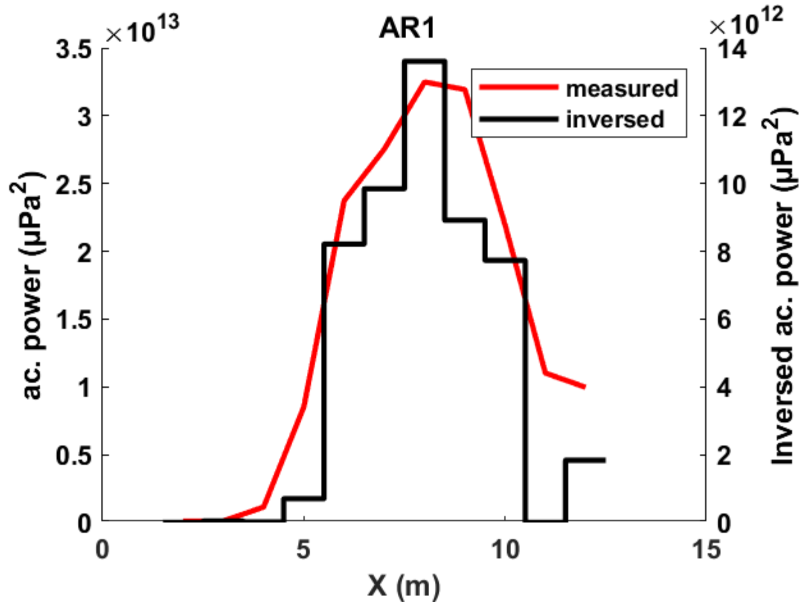

Figure S2

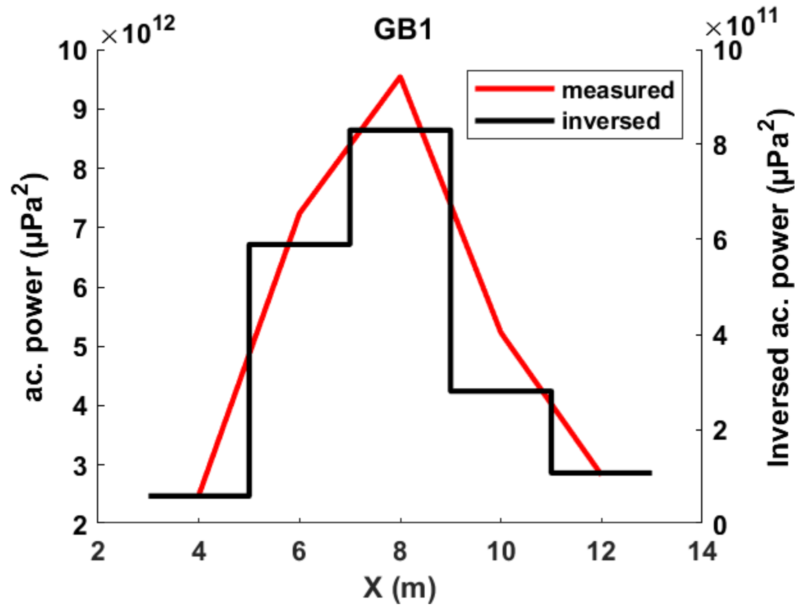

Figure S3

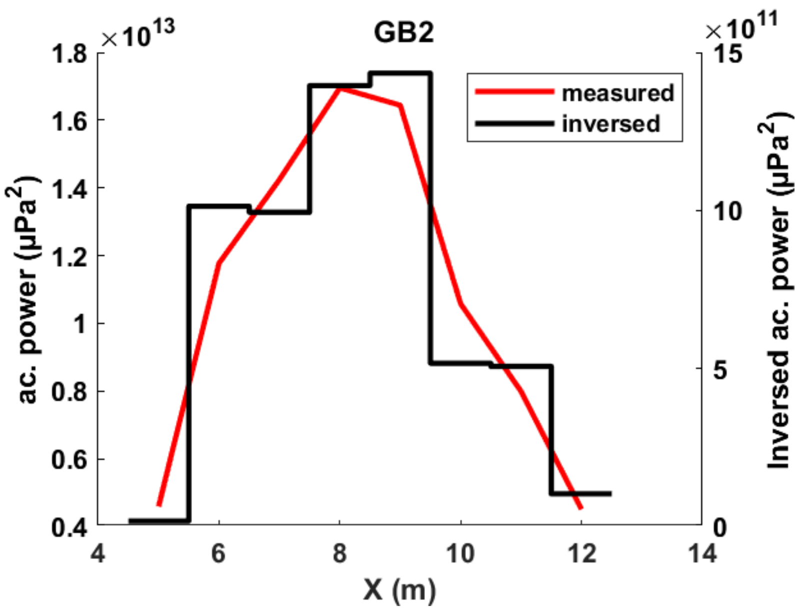

Figure S4

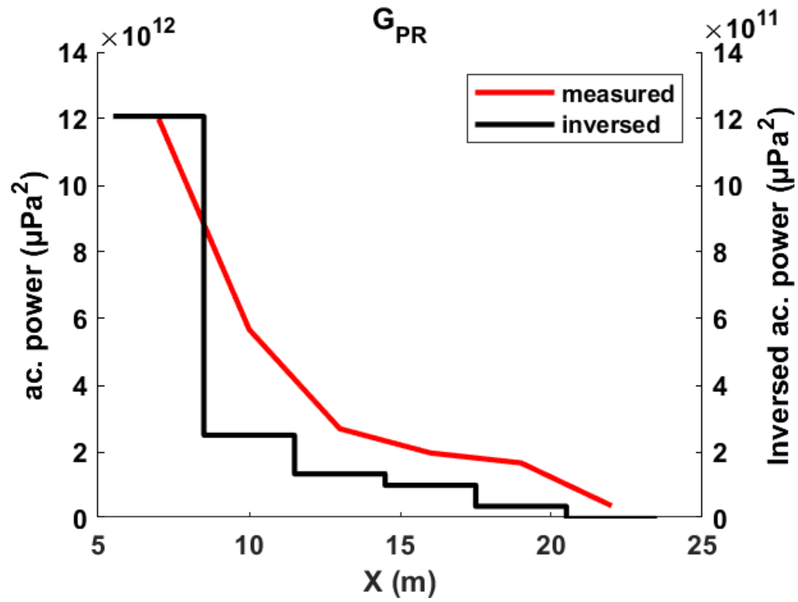

Figure S5

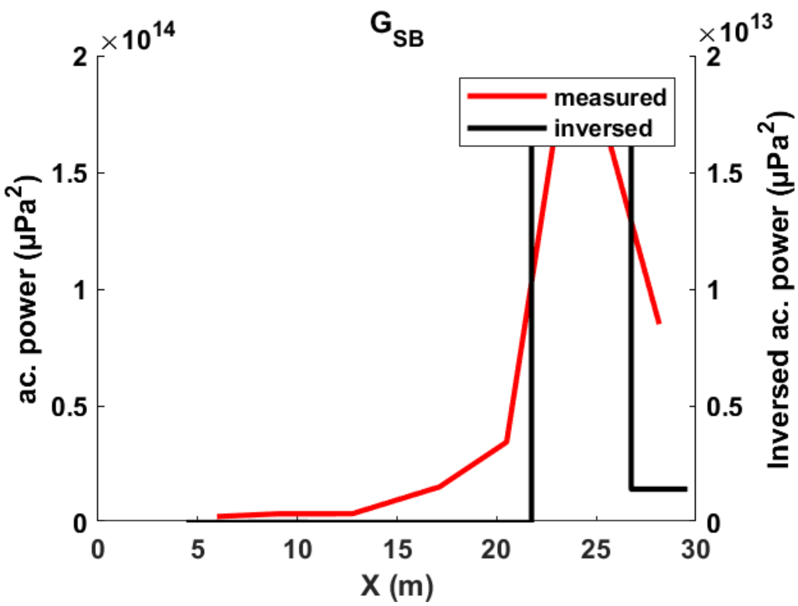

Figure S6

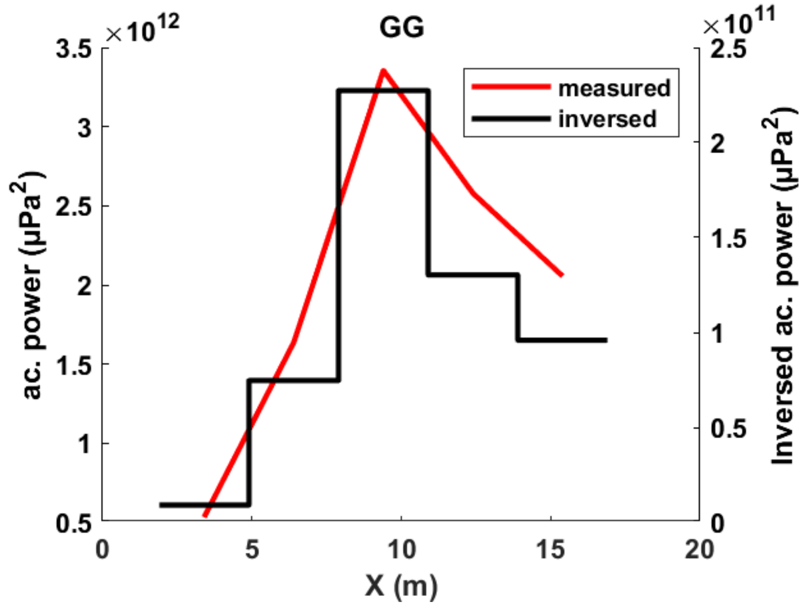

Figure S7

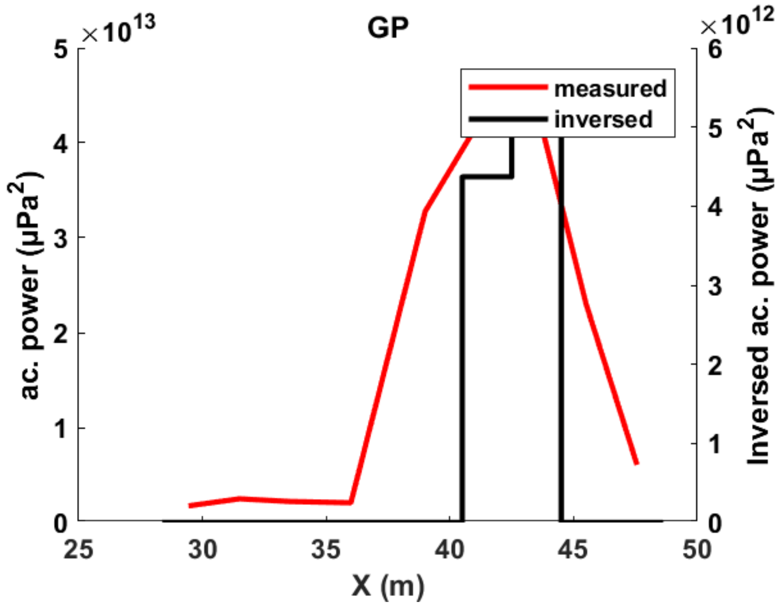

Figure S8

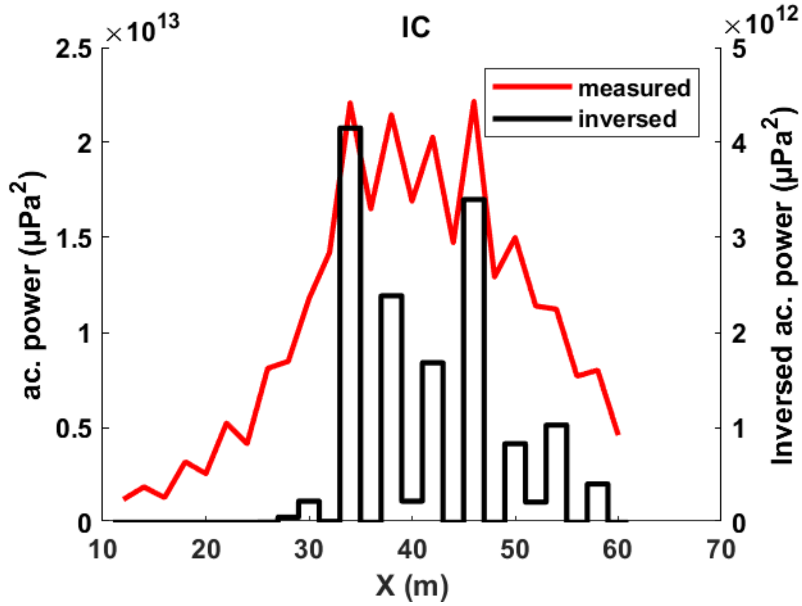

Figure S9

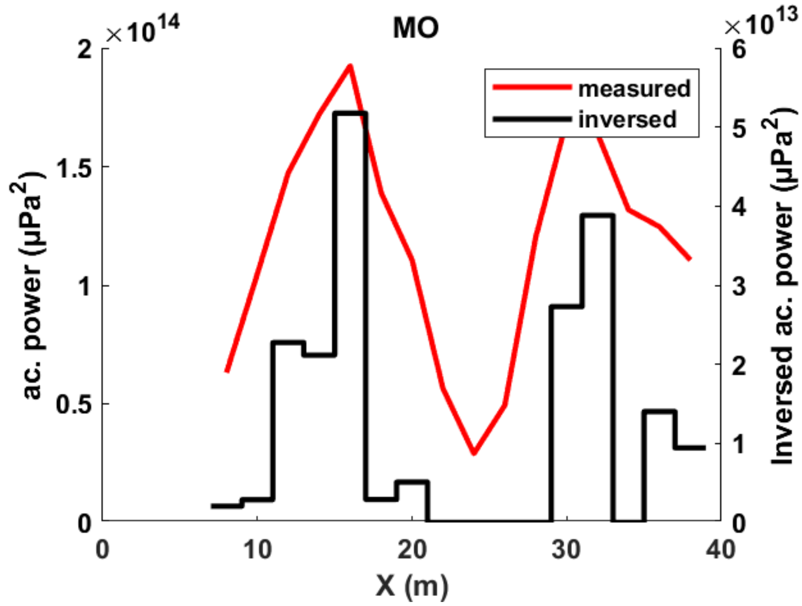

Figure S10

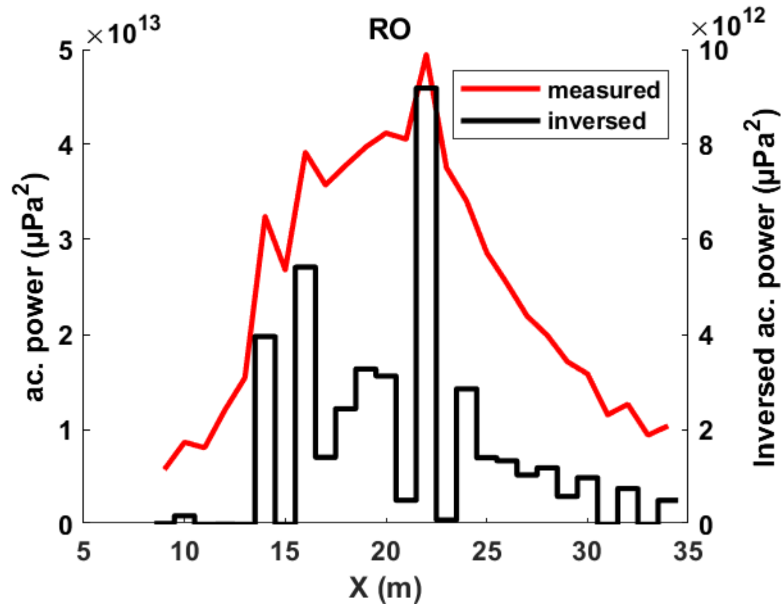

Figure S11

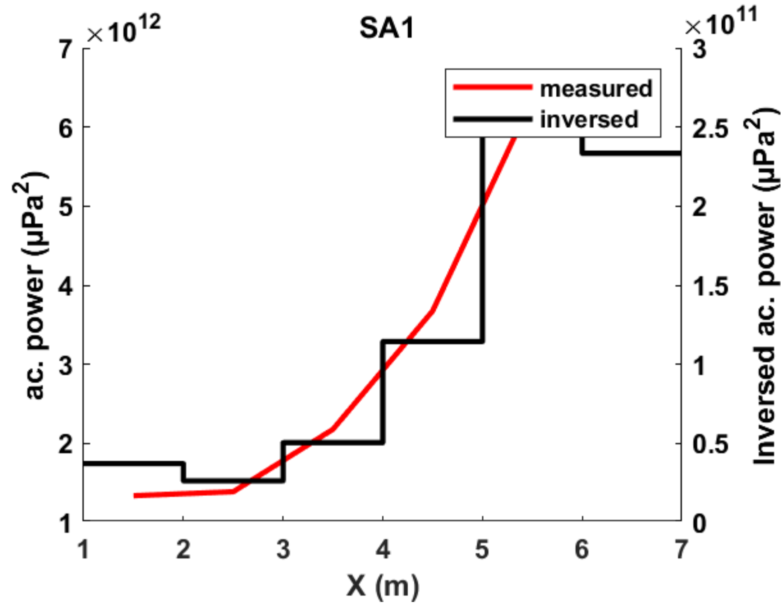

Figure S12

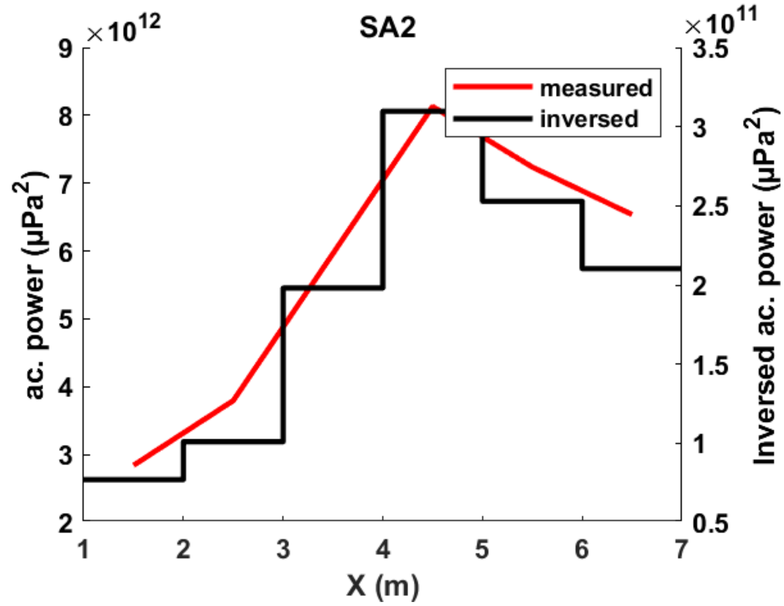

Figure S13

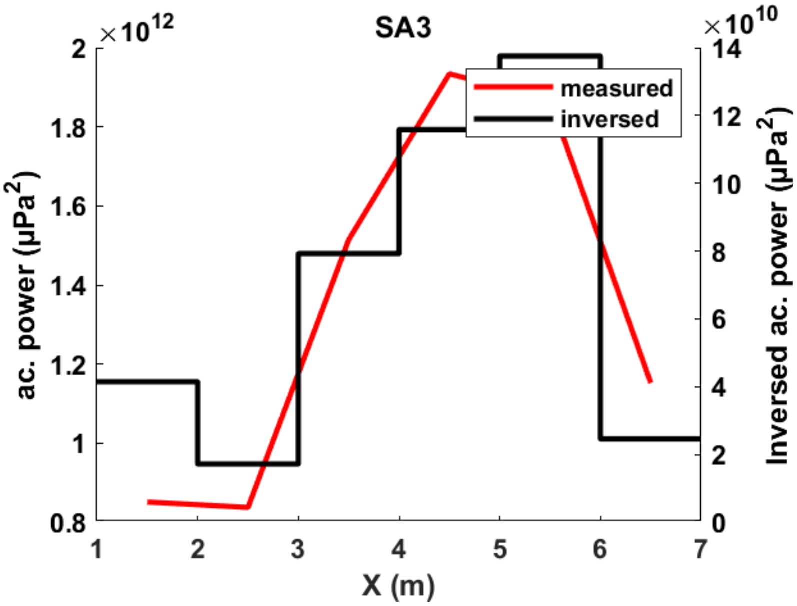

Figure S14

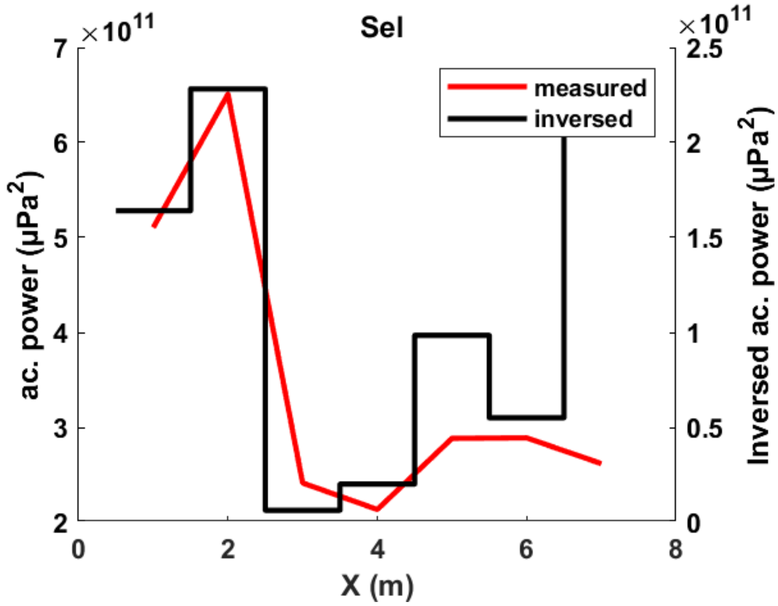

Figure S15

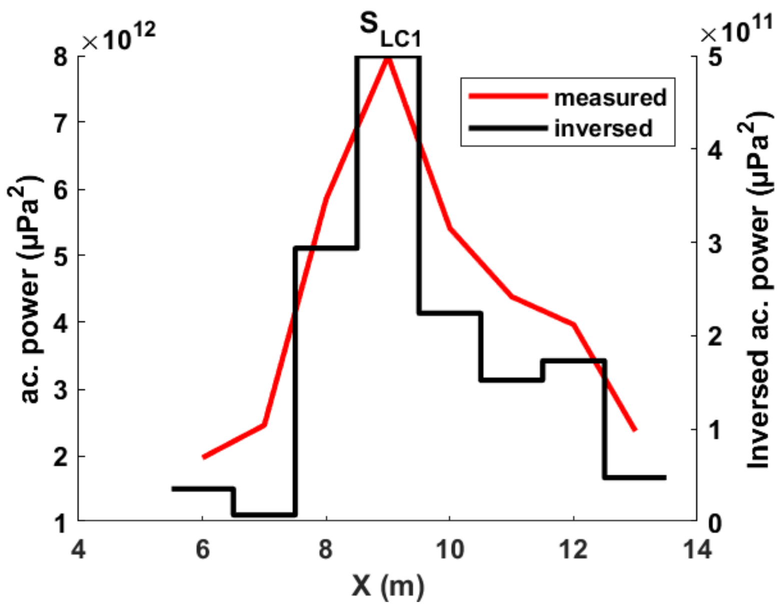

Figure S16

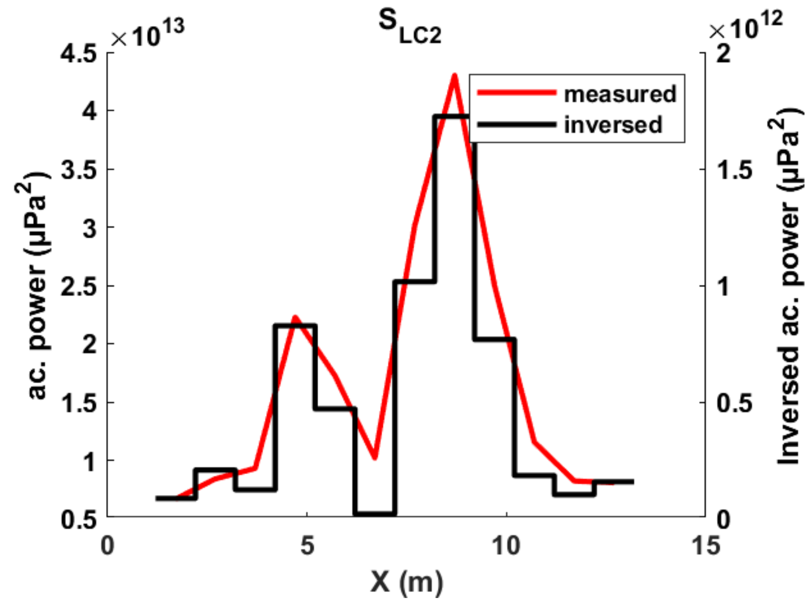

Figure S17

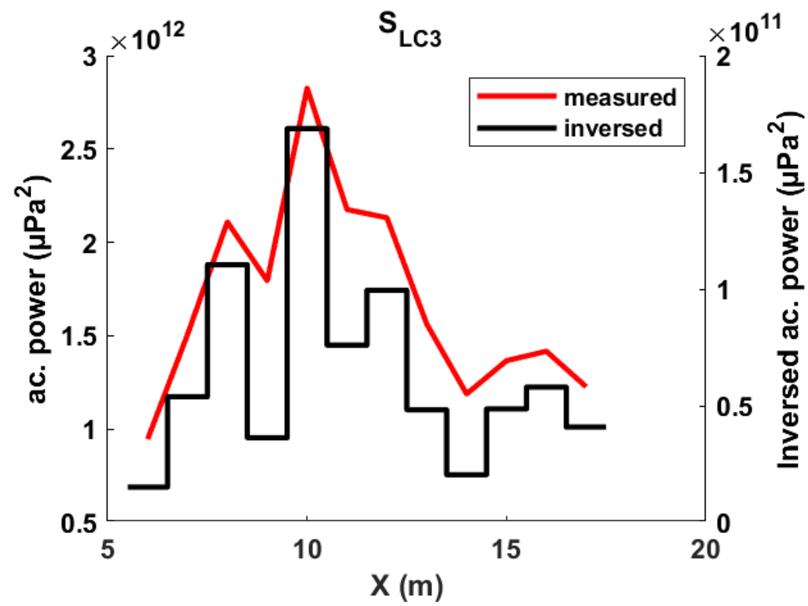

Figure S18

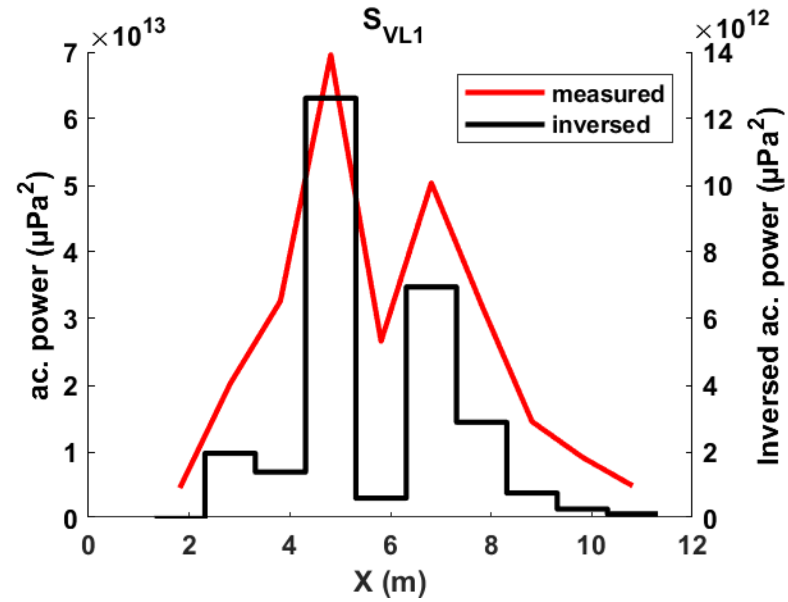

Figure S19

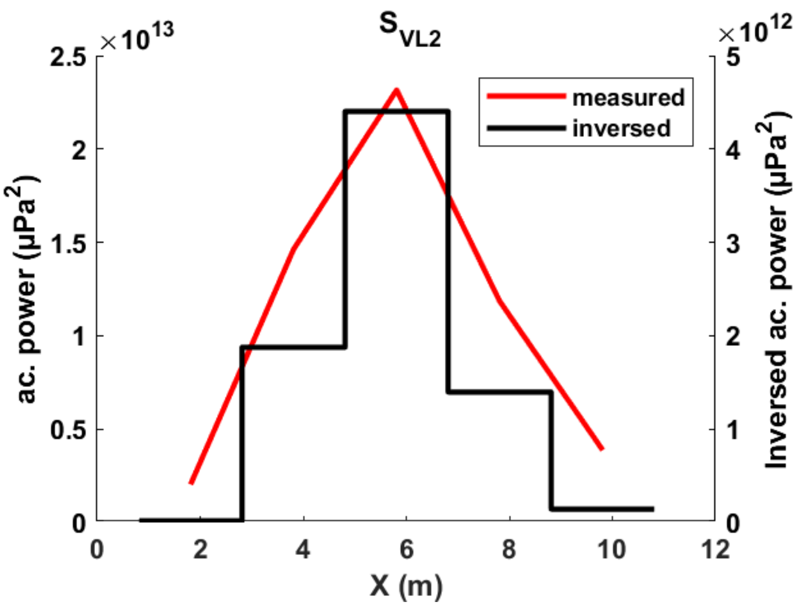

Figure S20

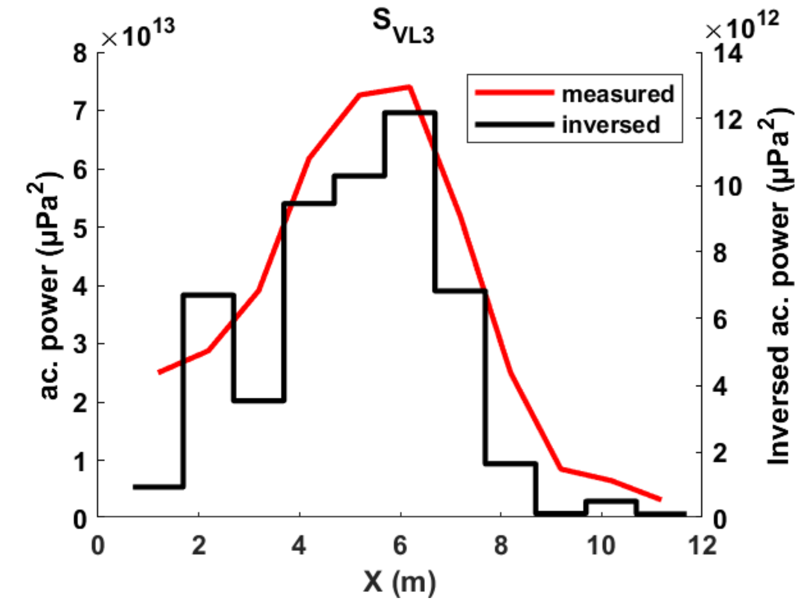

Figure S21

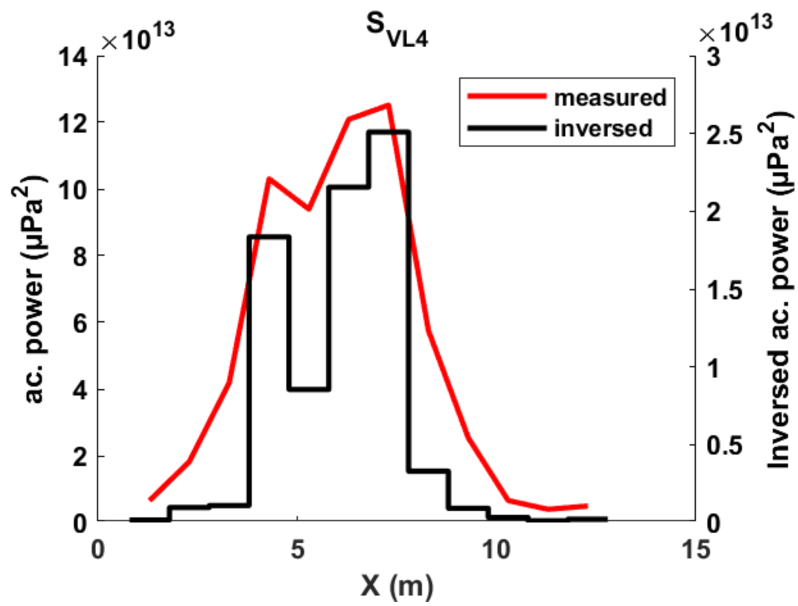

Figure S12

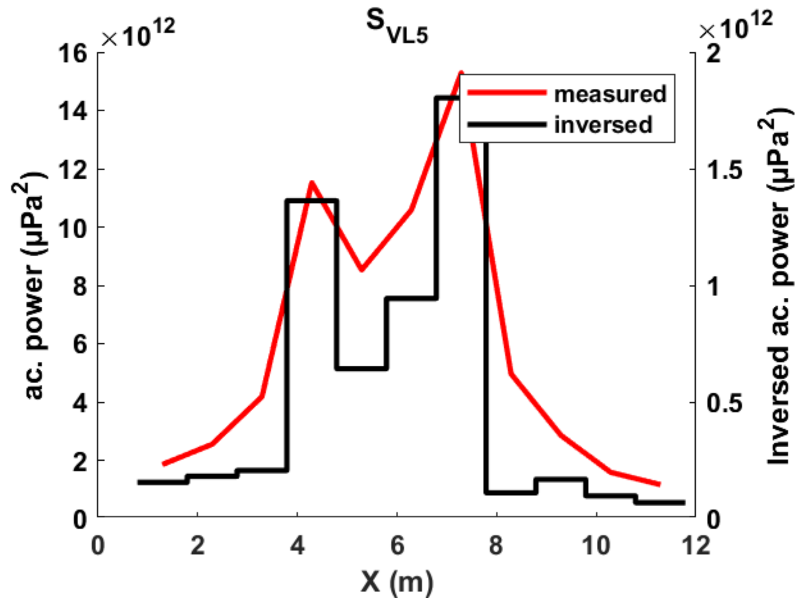

Figure S23

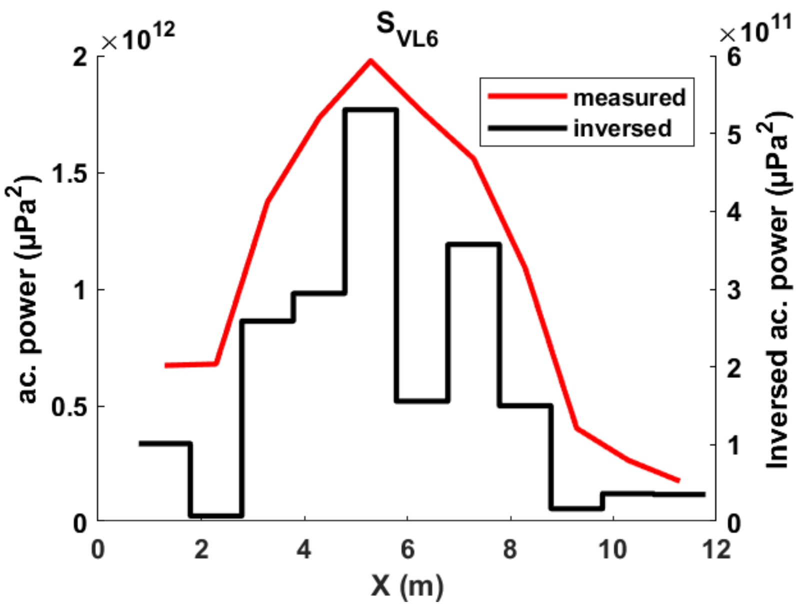

Figure S24

S2 Attenuation coefficient

In this section we present a river slope-based empirical equation to predict the attenuation coefficient of rives. The attenuation coefficients measured are best correlated with the local slope of the river (Geay et al., 2019). The fitted relation between slope and attenuation coefficient for both cylindrical ($\boldsymbol{\alpha_{\lambda,s}}$) and spherical ($\boldsymbol{\alpha_{\lambda,s}}$) model is presented in figure S25.

$$\alpha_c = 11.13S^{1.12} \tag{S1}$$

$$\alpha_s = 1181.29S^{2.2} \tag{S2}$$

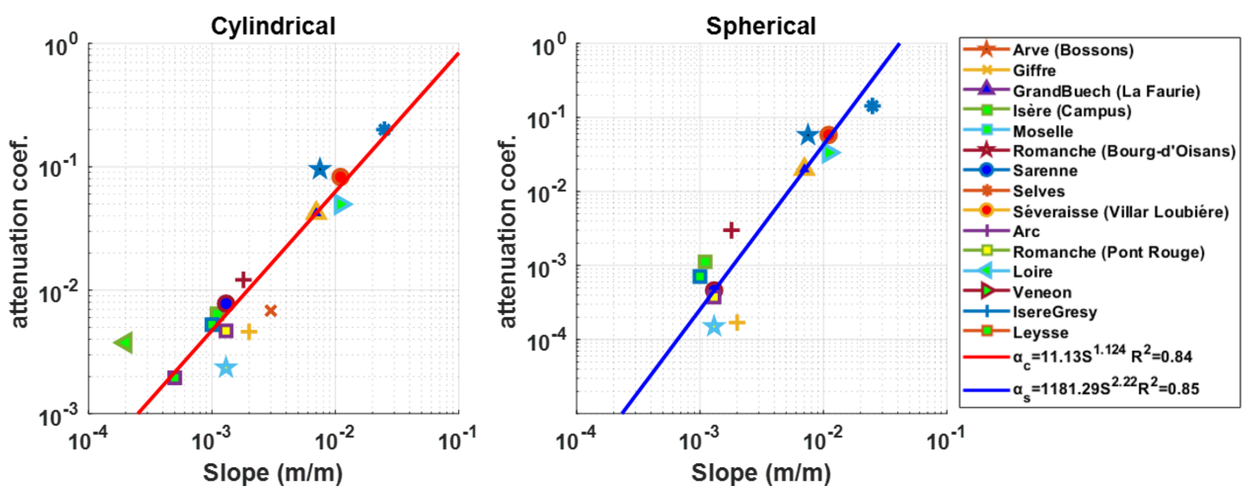

Figure S25. Relation between the local slope of the river and the attenuation coefficient for the cylindrical model (left) and spherical model (right)

Reference

Geay, T., Michel, L., Zanker, S., & Rigby, J. R. (2019). Acoustic wave propagation in rivers: an experimental study. *Earth Surface Dynamics*, *7*(2), 537–548. https://doi.org/10.5194/esurf-7-537-2019

Geay, T., Zanker, S., Misset, C., & Recking, A. (2020). Passive Acoustic Measurement of Bedload Transport: Toward a Global Calibration Curve? *Journal of Geophysical Research: Earth Surface*, *125*(8), e2019JF005242. https://doi.org/10.1029/2019JF005242